I&EC research
Industrial & Engineering Chemistry Research

Review

pubs.acs.org/IECR

Separation Performance of Graphene Oxide Membrane in Aqueous Solution

Di An, Ling Yang, Ting-Jie Wang,* and Boyang Liu

Department of Chemical Engineering, Tsinghua University, Beijing 100084, China

ABSTRACT: Graphene oxide (GO) is a type of two-dimensional nanomaterial with a single-atom thickness. GO sheets contain pristine regions, oxidized regions, and a small fraction of holes. By stacking GO sheets together, a GO membrane can be fabricated with sufficient mechanical strength. The interlayer nanocapillary network formed from connected interlayer spaces, together with the gaps between the edges of noninterlocked neighboring GO sheets and cracks or holes of the GO sheet, provides passage for molecules or ions to permeate through the GO membrane in an aqueous solution. The characteristics of molecules or ions (e.g., their size, charge, and the interaction with the GO membrane) affect the separation performance of the GO membrane. The contribution of gaps between neighboring GO sheets for separation can be adjusted by changing the GO sheet size and the GO membrane thickness. The interlayer space of the GO membrane can be adjusted by changing the water pH and modifying or reducing the GO sheets to obtain the desired separation performance. The production of the GO membrane is easily scalable and relatively inexpensive, indicating that the GO membrane has promising potential for applications such as water treatment, desalination, anticorrosion, chemical resistance, and controlled release coatings.

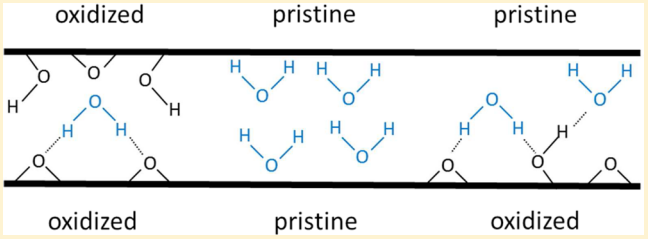

1. INTRODUCTION

Because of the scarcity of clean water and the increasingly serious water pollution, water treatment with membrane separation has attracted great attention. The extensive source and diverse species of molecules and ions in polluted water challenge the effective purification and separation of water by membranes. Recently, two-dimensional carbon-based materials such as graphene and, in particular, its derivative graphene oxide (GO), have brought new opportunities for membrane-based water treatment. Graphene is a single atomic sheet of sp^2 hybridized C atoms that is arranged in a honeycomb lattice and presents excellent mechanical strength,[1] high electrical conductivity,[2] superior thermal conductivity[3] and other fantastic properties, thus attracting considerable attention in various fields of research. The π-orbitals of graphene form a dense and delocalized electron cloud that blocks the voids within its aromatic rings.[4,5] Even the smallest molecule, He (its molecular radius is 1.3 Å), cannot permeate through a single graphene sheet.[6]

GO can be considered to be the oxidized form of graphene and was first prepared by Brodie[7] in 1859. The preparation method was then improved by Staudenmaier[8] and Hummers.[9] The conventional method for preparing GO is that natural graphite flakes are oxidized by using strong oxidants such as $KMnO_4$, $KClO_3$, or $NaNO_2$ in the presence of a strong acid, such as concentrated sulfuric acid or nitric acid. The individual GO sheets are exfoliated using ultrasonication. There are large amounts of oxygen-containing functional groups, including carboxyl, hydroxyl, epoxy, and carbonyl, on GO sheets due to oxidation,[10−13] as shown in Figure 1. The C/O ratio in GO, which indicates the degree of oxidation, can be quantified by elemental analysis or X-ray photoelectron spectroscopy (XPS), and the typical C/O ratio reported in the literature is 2−4.[11,12,14] When GO sheets are dispersed in water, the carboxyl and hydroxyl groups on the sheet are ionized and the GO sheets are highly negatively charged.[15] As a result, the electrostatic repulsion allows GO sheets to be easily dispersed in water (at concentrations up to 3 mg/mL),[16,17] forming stable, brown aqueous colloids. By vacuum filtrating, spin or

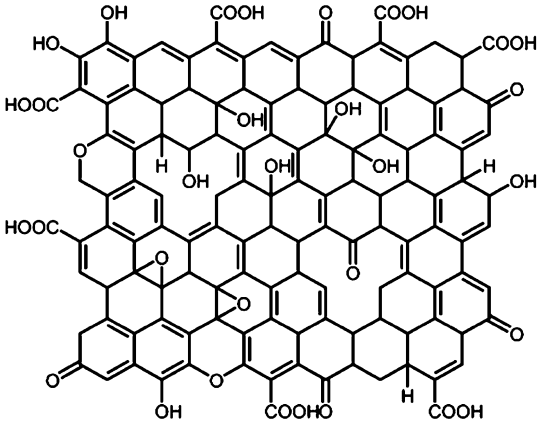

Figure 1. Structure of GO sheet. (Reproduced with permission from ref 12. Copyright 2015, Royal Society of Chemistry, London.)

Received: February 15, 2016
Revised: April 7, 2016
Accepted: April 8, 2016
Published: April 8, 2016

DOI: 10.1021/acs.iecr.6b00620
Ind. Eng. Chem. Res. 2016, 55, 4803−4810

spray coating of GO aqueous colloids, sheets stack together layer by layer. The strong interlayer hydrogen bonds between GO sheets hold them together to form a freestanding GO membrane with sufficient mechanical strength,[18] as shown in Figure 2.

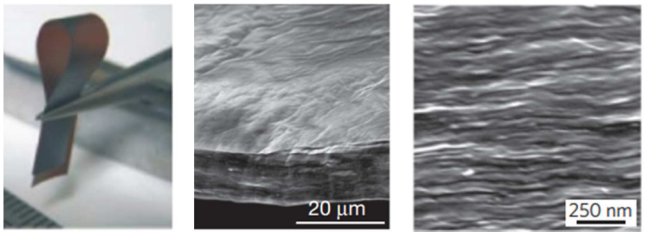

Figure 2. GO membrane and its cross section. (Reproduced with permission from ref 18. Copyright 2007, Macmillan Publishers, Ltd., New York.)

With the impermeability of GO sheets, small amounts of exfoliated sheets were dispersed into various types of polymers to fabricate the GO/polymer nanocomposites and thereby improve the barrier property of polymeric membranes in the gas phase.[19−22] With a novel separation mechanism, the GO membrane formed from stacked GO sheets exhibits excellent separation performance for different molecules and ions in an aqueous solution. Because GO membranes can be produced inexpensively on a large scale, they have great potential in applications of water treatment, desalination, anticorrosion, chemical resistance, and controlled release coatings. In this paper, recent progress concerning the separation performance of GO membranes in an aqueous solution was reviewed.

2. STRUCTURE OF THE GO MEMBRANE

A single GO sheet contains pristine regions, oxidized regions, and a small fraction of holes. The pristine region has the same structure as graphene, in which atoms are bonded in sp^2 hybridization. The oxidized region has a large amount of oxygen-containing functional groups, including carboxyl, hydroxyl, epoxy, and carbonyl, and the atoms are bonded in sp^3 hybridization.[11,23,24] XPS analysis can identify different types of carbon−oxygen bonds; the typical epoxy:hydroxyl:carbonyl:carboxyl ratio is 3−8:0.4−5:1−4:1.[25−29] During the aggressive oxidation and exfoliation of graphite, the partial carbon−carbon bonds of oxygen-containing functional groups linked on the GO sheets break. This releases CO and CO_2,[30] and holes on the order of 1−15 nm are formed.[31] The pristine and oxidized regions cover the majority of the GO sheet, with the discrete pristine regions being surrounded by the continuous oxidized regions. Erickson et al.[24] observed the structure of GO sheets by high-resolution transmission electron microscopy and found that the oxidized regions, pristine regions, and holes occurred at approximate percentages of 82%, 16%, and 2%, respectively, as shown in Figure 3.

Because of the existence of oxygen-containing functional groups on the GO sheets, the interlayer space of the GO membrane composed of stacked sheets is ∼6−7 Å under dry conditions, which is larger than the interlayer space of graphite of 3.4 Å. As the humidity increases, more water molecules diffuse into the interlayer between GO sheets, and the interlayer space of the GO membrane increases accordingly. When the GO membrane are immersed in water and fully wetted, the interlayer space increases to 12−13 Å.[32,33]

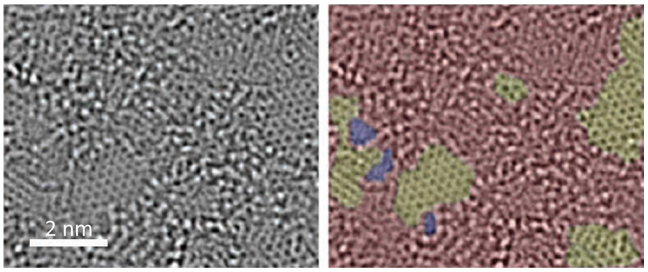

Figure 3. Aberration-corrected TEM images of GO sheet. (Reproduced with permission from ref 24. Copyright 2010, Wiley, New York.)

Considering that the water molecules are ∼3 Å in size, the interlayer spacing between the GO sheets being <7, 10, and 13 Å indicates that the layered structures of the water molecules should be in the form of a monolayer, bilayers, and trilayers, respectively.[34,35] Molecules and ions diffuse into the interlayer of the GO membrane from the edge of the GO sheets. The space between the GO sheets that form between two pristine regions face to face is large, thus allowing a fast diffusion rate for molecules and ions. In contrast, the space between the GO sheets that form between pristine and oxidized regions face to face is narrower. The narrower space and the interactions from hydrogen bonding and electrostatic interactions caused by oxidized regions that are randomly covered with, e.g., epoxy and hydroxyl groups, result in molecules and ions that are less mobile.[36,37] The space between the GO sheets with oxidized regions face to face is very narrow, thus blocking the diffusion of molecules and ions,[38,39] as shown in Figure 4. These

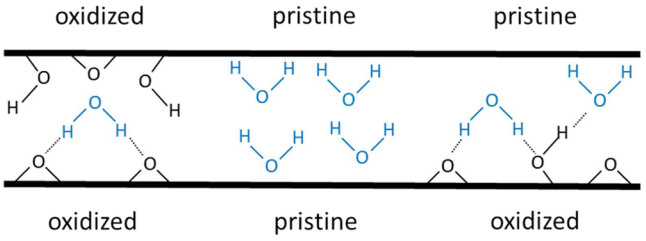

Figure 4. Interlayer structure of stacked GO membrane. (Reproduced with permission from ref 38. Copyright 2012, AAAS, Washington, DC.)

interlayer spaces connect and form networks of nanocapillaries between GO sheets, thereby providing passage for molecules and ions to diffuse in the direction parallel with the GO sheets.[38,40] Therefore, the separation mechanism of molecules and ions is primarily size exclusion from the interlayer space of nanocapillaries within the GO membrane. The interlayer space of the GO membrane can be adjusted for the requirements of specific applications by modifying or reducing the GO sheets utilizing the oxygen-containing functional groups.

Within the network of interlayer nanocapillaries, molecules and ions diffuse in the direction parallel to the GO sheets. At the gap between the edges of noninterlocked neighboring GO sheets[41] and at the cracks and holes on the sheet, molecules and ions diffuse in the direction vertical to the GO sheets and eventually permeate through the GO membrane. Therefore, in addition to the interlayer nanocapillaries, the gaps between noninterlocked neighboring GO sheets and the cracks and holes on the sheet affect the separation performance of the GO membrane. In addition, carboxyl and hydroxyl groups on GO

DOI: 10.1021/acs.iecr.6b00620
Ind. Eng. Chem. Res. 2016, 55, 4803−4810

sheets are ionized in water, which makes the GO sheets negatively charged. This affects the mobility of ions with different electric charges. The structure characteristics of the GO membrane result in effective separation for different molecules and ions. The selectivity is achieved by size exclusion from the interlayer space of the GO membrane, electrostatic interaction between different ions and negatively charged GO sheets, and ion adsorption including cation-π interaction and metal coordination to GO sheets, as shown in Figure 5.[12]

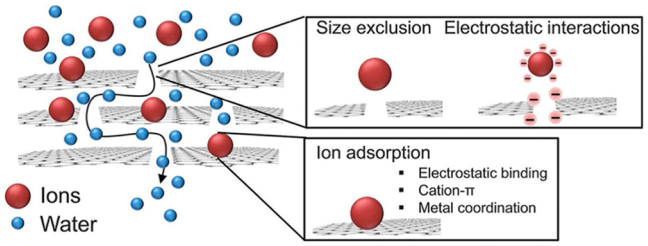

Figure 5. Separation of molecules and ions by GO membrane. (Reproduced with permission from ref 12. Copyright 2015, Royal Society of Chemistry, London.)

3. SEPARATION MECHANISM OF GO MEMBRANE

In the aqueous phase, water molecules can permeate through the GO membrane freely. Nair et al.[38] used a 0.5-μm-thick GO membrane to seal the open aperture of a metal container filled with water and detected the weight loss of the container due to water evaporation. It was found that the evaporation rate was almost the same as that without the GO membrane. This indicated that the GO membrane with 0.5 μm thickness did not significantly block the diffusion of water molecules. When the GO membrane was fully wetted, the interlayer space was measured to be a = 13 Å, from X-ray diffraction (XRD) analysis. Considering that the electronic clouds around graphene sheets extend over a distance of b = 3.4 Å, the interlayer space can be considered an empty space of width $\delta = a - b$ (or 9−10 Å), which is sufficient for water molecules to pass within the GO membrane. Nair et al.[38] calculated the moving velocity of water molecules through hydrophobic pristine region capillaries within the GO membrane by using molecular dynamics simulations and obtained a very high velocity of ~20 m/s. It was reasoned that the ultrafast diffusion rate of water molecules resulted from the high capillary pressure formed from the network of GO interlayer nanocapillaries and low-friction contact with the hydrophobic pristine region of GO sheets. The oxidized regions were considered spacers that could separate GO sheets by a certain distance. However, Wei et al.[36,37] reasoned that the oxidized regions not only take the role as spacers but also impede ultrafast water moving within GO membrane capillaries, because of the hydrogen bonds between water molecules and oxygen-containing groups. The fast permeation of water through the GO membrane was attributed mainly to its porous microstructures, such as the open space between the edges of neighboring GO sheets, the wide channels formed at wrinkles,[42] and holes on the GO sheets.

Because of size exclusion from the interlayer space within the GO membrane, molecules and ions can be separated according to their hydrated radius. Hung et al.[43] used the GO membrane to separate isopropyl alcohol from its aqueous solution with water containing 30 wt % by pervaporation. Isopropyl alcohol is blocked by the GO membrane, because its diameter is larger than the interlayer space. Because the GO membrane are permeable to water, the separation performance reached high efficiency, with the concentration of water obtained being ~99.5 wt %. The water flux changed little as the GO membrane thickness increased from 250 nm to 1 μm, indicating that the increase of GO membrane thickness had little effect on diffusion rate of water for relatively thin GO membranes. Joshi et al.[41] studied the penetration properties of molecules and ions at different sizes using a 5-μm-thick GO membrane. Because the interlayer space in the GO membrane in an aqueous phase was 9−10 Å,[38,43] the ions with a hydrated radius of >4.5 Å, e.g., $Ru(bipy)_3^{2+}$ ($Ru(C_{10}H_8N_2)_3^{2+}$), were sieved out by the GO membrane. However, species with a hydrated radius of <4.5 Å (e.g., K^+ and Mg^{2+}) can permeate through the GO membrane, as shown in Figure 6. The results from molecular dynamics

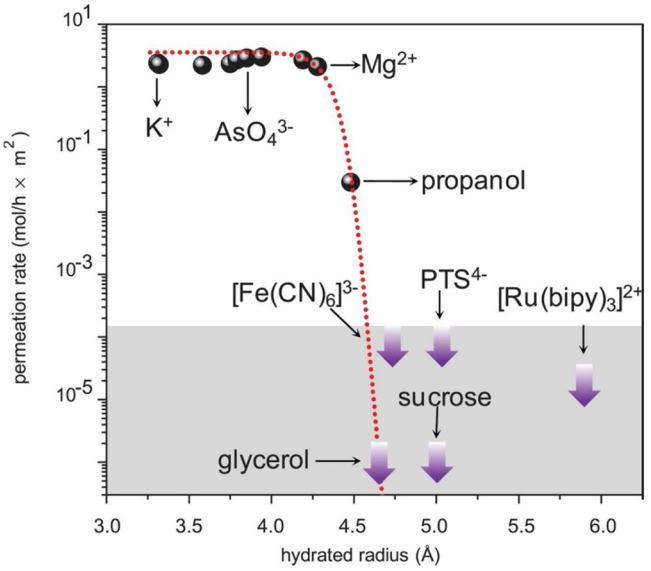

Figure 6. Permeation rates of molecules and ions with different sizes through the GO membrane. (Reproduced with permission from ref 41. Copyright 2014, AAAS, Washington, DC.)

simulations indicated that molecules and ions with smaller sizes were sucked inside the GO interlayer space, driven by the large capillary-like pressure formed from networks of GO interlayer nanocapillaries. As a result, the molecules and ions reached a high concentration (close to the saturation) inside the capillaries of the GO membrane. Therefore, smaller molecules and ions perform an ultrafast permeation through the GO membrane. Smaller ions such as Na^+ can permeate through the GO membrane and were measured to have diffusion rates thousands of times faster than what is expected for conventional diffusion.[41]

In addition to the hydrated radius of ions, both the ion charge and its interaction with GO sheets affect the separation performance of the GO membrane. Different anions and cations exhibit different permeation properties through the GO membrane. Sun et al.[44] studied the penetration properties of different anions through the GO membrane in different sodium salt solutions. The measured permeation rates were in the order of NaOH > $NaHSO_4$ > NaCl > $NaHCO_3$. For the NaOH solution, OH^- in the solution reacts with carboxyl and hydroxyl groups on GO sheets, which makes the sheets highly ionized. The electrostatic repulsion forces between GO sheets becomes

DOI: 10.1021/acs.iecr.6b00620
Ind. Eng. Chem. Res. 2016, 55, 4803−4810

large, and the interlayer space increases, thereby enabling OH^- and Na^+ ions to permeate quickly within the GO membrane. For the $NaHSO_4$ solution, because the H^+ cation in the solution prohibits the ionization of carboxyl and hydroxyl groups, the interlayer space of the GO membrane is relatively narrow, leading to a slow permeation of the ions. For the $NaHCO_3$ solution, the reaction between HCO_3^- and carboxyl groups on GO sheets leads to the generation of CO_2 gas, which hinders the permeation of ions.

Sun et al.[44,45] also measured the penetration rate of different transition-metal cations through the GO membrane, obtaining the following order of cations (based on penetration rate): $Mn^{2+} > Cd^{2+} > Cu^{2+}$. This resulted from the different strengths of coordination interactions between cations and GO sheets. The transition-metal cations (e.g., Fe^{3+}, Cu^{2+}, Cd^{2+}, Mn^{2+}) coordinate to sp^3 clusters in oxidized regions of GO sheets.[46,47] Sun et al.[48] used a GO membrane to filter the iron-based electrolytes containing $FeCl_3$ and HCl by the difference in the hydrated radius between Fe^{3+} (the hydrated radius is 4.57 Å) and H^+ (the hydrated radius is 2.82 Å) and the coordination interactions of Fe^{3+} with GO sheets. The measured permeation rate of H^+ was 2 orders of magnitude higher than that of Fe^{3+}. When the concentration of $FeCl_3$ in the electrolytes was <0.01 mol/L, the Fe^{3+} cation was blocked by GO membranes entirely, from which high-purity acids can be produced by circular penetration of electrolytes.

Alkali cations such as Na^+ and K^+ and alkaline-earth cations such as Mg^{2+}, Ca^{2+}, and Ba^{2+} lack d-orbital electrons and have no coordinated interactions with GO sheets. However, these cations can interact with sp^2 clusters in pristine regions of GO sheets through cation−π interactions, which are noncovalent interactions between cations and the aromatic π-electron cloud. The balance between cation−π interactions and the desolvation of the cations affect the permeation rate of cations through the GO membrane. The higher the solvation energy of cations, the weaker the cation-π interactions, because of the stronger screening effect of the hydration shell, resulting in permeation rates of anions in the following order: $Mg^{2+} > Na^+ > Ba^{2+}$, Ca^{2+}, K^+.[45] Because of the interactions between cations and GO sheets, small amounts of metal cations remained in the GO membrane after permeation, which were detected experimentally. However, as a result of repulsive forces between anions and the negatively charged GO sheets, the anions were not detected within the GO membrane after permeation.[44,45]

4. SEPARATION PERFORMANCE CONTROL OF GO MEMBRANE

4.1. Adjustment of GO Sheet Size and GO Membrane Thickness. Separation performance of GO membranes can be adjusted by changing the GO sheet size in the membrane preparation process. Sun et al.[45,48] produced nanosize GO sheets using wormlike graphite and microsize GO sheets using natural graphite and used them to prepare two different types of GO membranes. The permeation rate of molecules or ions through the GO membrane made from nanosized sheets is faster than that from microsized sheets, because more gaps exist between the edges of noninterlocked neighboring GO sheets in the GO membrane made from nanosized sheets than in the membrane made from microsized sheets. A larger number of gaps provide more passages for molecules and ions diffusing through the GO membrane in the direction vertical to the GO sheets. Therefore, the graphite type and size must be properly chosen in the preparation of GO membranes, with respect to the separation demands for different molecules and ions.

The separation performance of the GO membrane can also be adjusted by changing the thickness of the membrane. Coleman et al.[49] studied the penetration properties of $Ru(phen)_3^{2+}$ ($Ru(C_{12}H_8N_2)_3^{2+}$) and $Ru(bipy)_3^{2+}$ through GO membranes with different thicknesses. The two ions have almost the same ion charge, molecular weight, and diffusivity in water. Because $Ru(phen)_3^{2+}$ contains six extra C atoms, compared to $Ru(bipy)_3^{2+}$, the two ions had a subangstrom size difference, which caused the sterically hindered diffusion to differ. When the thickness of the GO membrane was <3 μm, the flow rate ratio of $Ru(phen)_3^{2+}$ to $Ru(bipy)_3^{2+}$ remained at a constant value of ∼0.65. However, when the thickness of the GO membrane was >3.5 μm, the flow rate ratio of the two ions decreased significantly to a value of 0.41. By constructing the steric hindrance diffusion model, ion penetration through the relatively thin GO membranes is mostly facilitated by the large pores (>1.75 nm in diameter) created by vacancies, edges, and cracks within individual GO sheets, whereas interlayer space formed by stacked GO sheet is dominant only in thick membranes. Because the GO membrane used by Joshi et al.[41] was considerably thick (5 μm), the penetration of $Ru(bipy)_3^{2+}$ through the membrane was mainly controlled by the interlayer space between GO sheets. As a result, the permeation of $Ru(bipy)_3^{2+}$ through the GO membrane was not detected. Thus, the separation ratio of different molecules or ions during preparation process can be adjusted readily by changing the quantity of stacked GO sheets, i.e., the thickness of the GO membrane.

4.2. Adjustment of Water pH. The ionization of the carboxyl and hydroxyl groups on GO sheets causes the sheets to become negatively charged. The degree of ionization can be adjusted by controlling the pH of water, and the separation performance of the GO membrane can be adjusted accordingly. Huang et al.[50] adjusted the water pH by adding sodium hydroxide and hydrochloric acid to adjust the water flux and rejection rate of Evans Blue ($C_{34}H_{24}N_6Na_4O_{14}S_4$) through the GO membrane. When the pH increased from 2 to 6, the zeta potential of GO sheets decreased, because of the increased degree of ionization of the carboxyl and hydroxyl groups, the increased electrostatic repulsion forces between GO sheets and the increased interlayer space between GO sheets, leading to an increased water flux and decreased rejection rate. When the pH was in the range of 6−8, the zeta potential of GO sheets changed little, thus, the water flux and rejection rate had no significant corresponding change. When the pH increased from 8 to 12, the zeta potential of GO sheets also changed slightly, but the electrical double layer screening effect predominated as the concentration of Na^+ increased in water, because of the addition of sodium hydroxide. This shrank the interspace distance of GO sheets, leading to a decrease in the water flux and increase of the rejection rate, as shown in Figure 7.

4.3. Composite and Modification of GO Membrane. The separation performance of the GO membrane can also be adjusted by fabricating different GO membrane structures by utilizing the oxygen-containing functional groups on GO sheets. Huang et al.[51] prepared a composite membrane by filtering a mixture solution of negatively charged GO sheets and positively charged $Cu(OH)_2$ nanostrands. After the nanostrands were dissolved using an acid solution, numerous nanochannels with diameters of 3−5 nm were formed in the membrane, which was larger than the interlayer space of the

DOI: 10.1021/acs.iecr.6b00620
Ind. Eng. Chem. Res. 2016, 55, 4803−4810

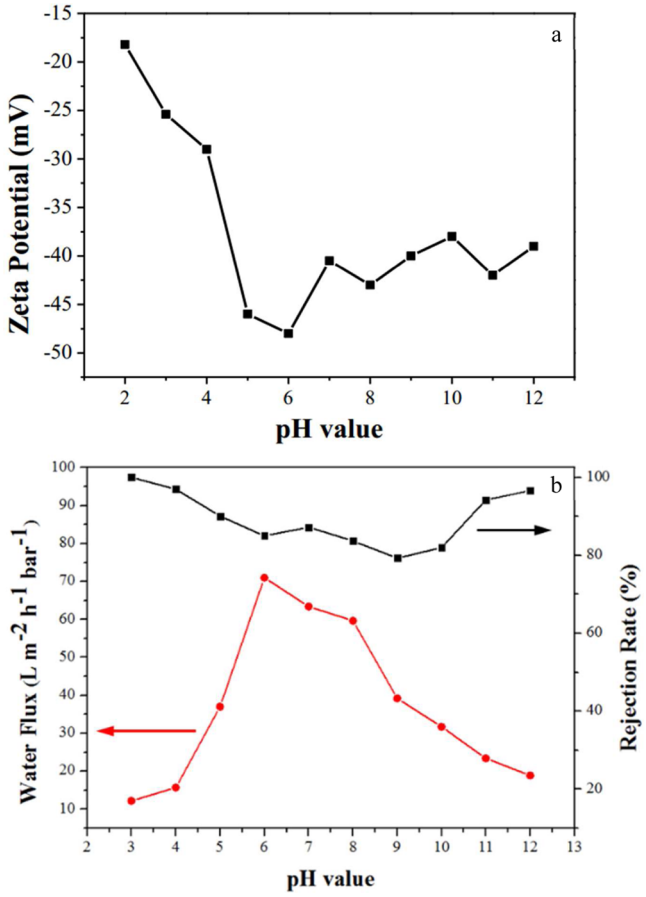

Figure 7. pH effects on the separation performance of Evans Blue using GO membrane: (a) zeta potential of GO sheets and (b) water flux and rejection rate of Evans Blue. (Reproduced with permission from ref 50. Copyright 2013, Royal Society of Chemistry, London.)

original GO membrane. The water permeation rate in nanochanneled GO membrane was 10 times higher than that in the original one, without compromising the rejection rate of dye molecules such as Rhodamine B ($C_{28}H_{31}ClN_2O_3$) and Evans Blue. Wang et al.[52] fabricated a GO membrane with nanosized carbon dots embedded inside to adjust the interlayer space of the membrane. By adding carbon dots with different sizes controlled precisely, a 2- to 9-fold increase in the water permeation rate was obtained, and the removal efficiency of Rhodamine B, Methylene Blue ($C_{16}H_{18}ClN_3S$), and Methyl Orange ($C_{14}H_{14}N_3SO_3Na$) reached >99% and changed little.

Li et al.[53] added the water-soluble material poly(vinylpyrrolidone) in the interlayer of the GO membrane to increase the interlayer space and increased the permeation rate of Reactive Red X-3B ($C_{19}H_{10}Cl_2N_6Na_2O_7S_2$) through the GO membrane. Jia et al.[54] prepared covalently cross-linked GO membranes using dicarboxylic acids with different chain lengths using esterification reactions. Because of the cross-linking between GO sheets, the elastic moduli of the GO membranes increased significantly. The interlayer space generally increased with the chain length, and the permeation rate of KCl and $K_4Fe(CN)_6$ through GO membranes increased correspondingly. Thus, the interlayer space of the GO membrane can be enlarged by fabricating the membrane utilizing the oxygen-containing functional groups on GO sheets. The water flux was increased significantly through the GO membrane without compromising the rejection rate of large ions or molecules for high-efficiency applications involving water separation and purification.

4.4. Reduction of GO Membrane. Reduction of the GO membrane can eliminate the oxygen-containing functional groups on GO sheets, thus reducing the interlayer space between GO sheets and increasing the barrier properties of the membrane. Many methods can be used to reduce the GO membrane, e.g., using strong reductants such as hydrazine,[13,55,56] vitamin C,[57,58] hydroxylamine,[59] or HI acid,[60] as well as treatment under hydrothermal conditions.[61] XPS or elemental analysis is commonly employed to analyze the reduction degree. After reduction, the C/O ratio of GO increased to ~12 in most cases.[62,63] Raman spectrometry is also widely used to examine the reduction characteristics. The D-band (peak at ~1320−1350 cm^{-1}) and G-band (peak at ~1570−1585 cm^{-1}) are the main characteristic bands in the Raman spectra of GO and reduced GO. The increase of the ratio of D- and G-band intensity (I_D/I_G) in reduced GO, compared to that in GO, indicates that the reduction occurs.[64,65] Nair et al.[38] reduced the GO membrane by annealing at 250 °C in a hydrogen−argon atmosphere. The interlayer space of the membrane decreased from 10 Å to 4 Å, and no water vapor permeation through the reduced GO membrane was detected. Su et al.[66] reduced GO membranes by thermal reduction, vitamin C solution, and HI acid vapor to obtain T-RGO, VC-RGO, and HI-RGO membranes, respectively. The interlayer spaces of T-RGO and VC-RGO decreased to 4 Å, and that of HI-RGO was ~3.6 Å, which was close to the interlayer space in graphite. Because of the decrease in interlayer space, the T-RGO and VC-RGO membranes exhibited water permeation rate decreases of 3 and 5 orders of magnitude, respectively, compared with the original GO membrane. The decrease in interlayer space provided a stronger barrier in HI-RGO membrane, through which water permeation was not detected. Su et al.[66] produced GO membranes by drop casting on the surface of metals, e.g., Cu and Ni. After reduction by vitamin C, subsequently, concentrated nitric acid or hydrochloric acid was deposited dropwise on the VC-RGO membrane, but no degradation of the surface was observed after several days, indicating that RGO membranes can be used as an anticorrosion and chemical-resistant coating.

Liu et al.[67] reduced the GO membrane using HI acid vapor. After reduction, the hydrophobicity of the membrane increased, and the water contact angle increased from 38° to 78°. Compared to the original GO membrane, the NaCl rejection rate of the reduced membrane was increased. Neither Cu^{2+} nor Acid Orange 7 ($C_{16}H_{11}N_2NaO_4S$) was detected while passing through the reduced GO membrane. Sun et al.[68] intercalated monolayer titania nanosheets, which were prepared by delaminating layered titanates into single molecular sheets[69,70] and into the GO sheets to form the hybrid membrane. GO sheets then were reduced under ultraviolet irradiation by utilizing photocatalytic properties of titania nanosheets. With a gradual increase in both the titania nanosheet content within the membrane and the irradiation time under UV light, the reduction degree of GO sheets increased, and the sheets became more flattened. The number of nanocapillaries for ions diffusing within them decreased, and the permeation rate of Na^+ through the membrane eventually decreased. Zhang et al.[71] mechanically coated GO membranes on KNO_3 fertilizer pellets that were subsequently thermally reduced. The pellets were immersed in water to measure the release property, and the

DOI: 10.1021/acs.iecr.6b00620
Ind. Eng. Chem. Res. 2016, 55, 4803−4810

release duration of the pellets was extended, compared with uncoated fertilizer. This indicates that the reduced GO membrane can be used as coating material for controlled-release fertilizer.

5. STABILITY OF GO MEMBRANE IN AQUEOUS SOLUTION

As a type of nanomaterial, GO was reported to have potential risks to environment and human health.[72,73] The cytotoxicity of GO is dependent on its size,[74] the degree of oxidation,[75] and the dosages on cells or bacteria,[76] etc. The disengagement of GO sheets from the GO membrane in applications would cause potential pollution to aqueous environment, so stability of the GO membrane in aqueous solution is crucial.

However, because of the highly hydrophilic nature of the GO sheet, the GO membrane soaked in water will disintegrate over time[77−79] (e.g., the GO membrane prepared by Yeh et al.[78] using a vacuum filtration method was completely redispersed in pure water after 1 day), while the GO membrane was very stable in a high-concentration salt solution, even under ultrasonic treatment.[79] This is because the interactions between water molecules and GO are weakened and the electrostatic repulsion between GO sheets is decreased, because of the existence of salt ions in aqueous solution. Taking advantage of the oxygen-containing functional groups on GO sheets, adjacent GO sheets could be chemical cross-linked by divalent metal ions[47,78] or organic molecules such as dicarboxylic acids[54] and amines[25,80,81] etc., thus improving the stability of GO membrane. Yeh et al.[78] prepared GO membranes via a vacuum filtration method, using a porous anodized aluminum oxide (AAO) filter disk, which is the most commonly used filter disk. During the filtration of the acidic GO solution, the AAO filter disk corroded to release a small amount of Al^{3+}, which cross-linked the GO sheets, so the GO membrane becomes very stable in stirred pure water. Huang et al.[25] selected poly(ethylenimine) as the cross-linker to prepare GO membranes; the integrity of the membrane was maintained after oscillation for 1 day in water and the water remained clear and clean, which indicated the excellent stability. The reduced GO membrane exhibits high stability for a long time in aqueous solution, the stability is attributed to the enhancement of the $\pi-\pi$ interactions between reduced GO sheets.[12,82] Although the stability of GO membrane could be improved in different approach, further research on long-term stability should be pursued.

6. CONCLUSIONS

The graphene oxide (GO) membrane shows excellent separation performance for different molecules and ions. The interlayer nanocapillary networks formed due to the connected interlayer spaces, together with the gaps between edges of noninterlocked neighboring GO sheets and the cracks or holes of the GO sheet, provide passage for molecules or ions to permeate through the GO membrane in aqueous solutions, achieving the effective separation of different molecules and ions. Many factors, including the size of the molecules or ions, the charge of the ions, and interactions such as electrostatic interaction, metal coordination, and cation$-\pi$ interaction between ions and GO sheets affect the separation performance of the GO membrane. The molecules or ions with smaller hydrated radius, less charge, and weaker interaction with GO sheets permeate through the GO membrane more easily. Driven by the high capillary-like pressure resulting from the nanocapillary network in the GO membrane, molecules or ions with smaller sizes undergo an ultrafast permeation through the GO membrane, whereas those with larger size are blocked and separated.

The GO membrane has promising potential in the applications of water treatment, especially the removal of toxic ions and organic molecules in polluted water. The desired separation performance with high water flux and rejection rates can be achieved by adjusting the GO sheet size, the thickness of the GO membrane, water pH, and the GO membrane structure. The GO membrane also have potential applications in the fields of anticorrosion, chemical resistance, and controlled release coating, because of the impermeability of the reduced GO membrane. For environmental benign and practical applications, further research focused on improving long-term stability of GO membrane in aqueous solution is of great importance. Thorough ecotoxicological assessments on applying GO should be further studied, in order to effectively utilize the unique properties of GO membrane and eliminate the possible associated adverse health and environmental effects.

AUTHOR INFORMATION

Corresponding Author

*Tel.: +86-10-62788993. Fax: +86-10-62772051. E-mail: wangtj@tsinghua.edu.cn.

Notes

The authors declare no competing financial interest.

ACKNOWLEDGMENTS

The authors wish to express their appreciation for the financial support of this study by the National Natural Science Foundation of China (NSFC No. 20876085).

REFERENCES

(1) Lee, C.; Wei, X.; Kysar, J. W.; Hone, J. Measurement of the elastic properties and intrinsic strength of monolayer graphene. *Science* **2008**, *321*, 385−388.
(2) Jung, I.; Dikin, D. A.; Piner, R. D.; Ruoff, R. S. Tunable electrical conductivity of individual graphene oxide sheets reduced at "low" temperatures. *Nano Lett.* **2008**, *8*, 4283−4287.
(3) Balandin, A. A.; Ghosh, S.; Bao, W.; Calizo, I.; Teweldebrhan, D.; Miao, F.; Lau, C. N. Superior thermal conductivity of single-layer graphene. *Nano Lett.* **2008**, *8*, 902−907.
(4) Berry, V. Impermeability of graphene and its applications. *Carbon* **2013**, *62*, 1−10.
(5) Sreeprasad, T. S.; Berry, V. How do the electrical properties of graphene change with its functionalization? *Small* **2013**, *9*, 341−350.
(6) Bunch, J. S.; Verbridge, S. S.; Alden, J. S.; Van der Zande, A. M.; Parpia, J. M.; Craighead, H. G.; McEuen, P. L. Impermeable atomic membranes from graphene sheets. *Nano Lett.* **2008**, *8*, 2458−2462.
(7) Brodie, B. C. On the atomic weight of graphite. *Philos. Trans. R. Soc. London* **1859**, *149*, 249−259.
(8) Staudenmaier, L. Verfahren zur darstellung der graphitsäure. *Ber. Dtsch. Chem. Ges.* **1898**, *31*, 1481−1487.
(9) Hummers, W. S.; Offeman, R. E. Preparation of graphitic oxide. *J. Am. Chem. Soc.* **1958**, *80*, 1339−1339.
(10) He, H.; Klinowski, J.; Forster, M.; Lerf, A. A new structural model for graphite oxide. *Chem. Phys. Lett.* **1998**, *287*, 53−56.
(11) Dreyer, D. R.; Park, S.; Bielawski, C. W.; Ruoff, R. S. The chemistry of graphene oxide. *Chem. Soc. Rev.* **2010**, *39*, 228−240.
(12) Perreault, F.; Fonseca de Faria, A.; Elimelech, M. Environmental applications of graphene-based nanomaterials. *Chem. Soc. Rev.* **2015**, *44*, 5861−5896.

DOI: 10.1021/acs.iecr.6b00620
Ind. Eng. Chem. Res. 2016, 55, 4803−4810

(13) Stankovich, S.; Piner, R. D.; Chen, X.; Wu, N.; Nguyen, S. T.; Ruoff, R. S. Stable aqueous dispersions of graphitic nanoplatelets via the reduction of exfoliated graphite oxide in the presence of poly (sodium 4-styrenesulfonate). *J. Mater. Chem.* **2006**, *16*, 155−158.
(14) Kim, H.; Abdala, A. A.; Macosko, C. W. Graphene/polymer nanocomposites. *Macromolecules* **2010**, *43*, 6515−6530.
(15) Li, D.; Mueller, M. B.; Gilje, S.; Kaner, R. B.; Wallace, G. G. Processable aqueous dispersions of graphene nanosheets. *Nat. Nanotechnol.* **2008**, *3*, 101−105.
(16) Stankovich, S.; Piner, R. D.; Nguyen, S. T.; Ruoff, R. S. Synthesis and exfoliation of isocyanate-treated graphene oxide nanoplatelets. *Carbon* **2006**, *44*, 3342−3347.
(17) Park, S.; Ruoff, R. S. Chemical methods for the production of graphenes. *Nat. Nanotechnol.* **2009**, *4*, 217−224.
(18) Dikin, D. A.; Stankovich, S.; Zimney, E. J.; Piner, R. D.; Dommett, G. H. B.; Evmenenko, G.; Nguyen, S. T.; Ruoff, R. S. Preparation and characterization of graphene oxide paper. *Nature* **2007**, *448*, 457−460.
(19) Kim, H.; Miura, Y.; Macosko, C. W. Graphene/polyurethane nanocomposites for improved gas barrier and electrical conductivity. *Chem. Mater.* **2010**, *22*, 3441−3450.
(20) Tsai, M. H.; Tseng, I.; Liao, Y. F.; Chiang, J. C. Transparent polyimide nanocomposites with improved moisture barrier using graphene. *Polym. Int.* **2013**, *62*, 1302−1309.
(21) Huang, H. D.; Ren, P. G.; Chen, J.; Zhang, W. Q.; Ji, X.; Li, Z. M. High barrier graphene oxide nanosheet/poly(vinyl alcohol) nanocomposite films. *J. Membr. Sci.* **2012**, *409-410*, 156−163.
(22) Kim, H. M.; Lee, J. K.; Lee, H. S. Transparent and high gas barrier films based on poly(vinyl alcohol)/graphene oxide composites. *Thin Solid Films* **2011**, *519*, 7766−7771.
(23) Cai, W. W.; Piner, R. D.; Stadermann, F. J.; Park, S.; Shaibat, M. A.; Ishii, Y.; Yang, D. X.; Velamakanni, A.; An, S. J.; Stoller, M.; An, J.; Chen, D.; Ruoff, R. S. Synthesis and solid-state NMR structural characterization of ^{13}C-labeled graphite oxide. *Science* **2008**, *321*, 1815−1817.
(24) Erickson, K.; Erni, R.; Lee, Z.; Alem, N.; Gannett, W.; Zettl, A. Determination of the local chemical structure of graphene oxide and reduced graphene oxide. *Adv. Mater.* **2010**, *22*, 4467−4472.
(25) Huang, T.; Zhang, L.; Chen, H.; Gao, C. Sol-gel fabrication of a non-laminated graphene oxide membrane for oil/water separation. *J. Mater. Chem. A* **2015**, *3*, 19517−19524.
(26) Seo, M.; Yoon, D.; Hwang, K. S.; Kang, J. W.; Kim, J. Supercritical alcohols as solvents and reducing agents for the synthesis of reduced graphene oxide. *Carbon* **2013**, *64*, 207−218.
(27) Mattevi, C.; Eda, G.; Agnoli, S.; Miller, S.; Mkhoyan, K. A.; Celik, O.; Mastrogiovanni, D.; Granozzi, G.; Garfunkel, E.; Chhowalla, M. Evolution of electrical, chemical, and structural properties of transparent and conducting chemically derived graphene thin films. *Adv. Funct. Mater.* **2009**, *19*, 2577−2583.
(28) Tu, Y.; Ichii, T.; Utsunomiya, T.; Sugimura, H. Vacuum-ultraviolet photoreduction of graphene oxide: Electrical conductivity of entirely reduced single sheets and reduced micro line patterns. *Appl. Phys. Lett.* **2015**, *106*, 133105.
(29) Compton, O. C.; Dikin, D. A.; Putz, K. W.; Brinson, L. C.; Nguyen, S. T. Electrically conductive "alkylated" graphene paper via chemical reduction of amine-functionalized graphene oxide paper. *Adv. Mater.* **2010**, *22*, 892−896.
(30) Paci, J. T.; Belytschko, T.; Schatz, G. C. Computational studies of the structure, behavior upon heating, and mechanical properties of graphite oxide. *J. Phys. Chem. C* **2007**, *111*, 18099−18111.
(31) Gomez-Navarro, C.; Meyer, J. C.; Sundaram, R. S.; Chuvilin, A.; Kurasch, S.; Burghard, M.; Kern, K.; Kaiser, U. Atomic structure of reduced graphene oxide. *Nano Lett.* **2010**, *10*, 1144−1148.
(32) Buchsteiner, A.; Lerf, A.; Pieper, J. Water dynamics in graphite oxide investigated with neutron scattering. *J. Phys. Chem. B* **2006**, *110*, 22328−22338.
(33) Lerf, A.; Buchsteiner, A.; Pieper, J.; Schöttl, S.; Dekany, I.; Szabo, T.; Boehm, H. P. Hydration behavior and dynamics of water molecules in graphite oxide. *J. Phys. Chem. Solids* **2006**, *67*, 1106−1110.
(34) Talyzin, A. V.; Luzan, S. M.; Szabo, T.; Chernyshev, D.; Dmitriev, V. Temperature dependent structural breathing of hydrated graphite oxide in H_2O. *Carbon* **2011**, *49*, 1894−1899.
(35) Boukhvalov, D. W.; Katsnelson, M. I.; Son, Y. W. Origin of anomalous water permeation through graphene oxide membrane. *Nano Lett.* **2013**, *13*, 3930−3935.
(36) Wei, N.; Peng, X.; Xu, Z. Understanding water permeation in graphene oxide membranes. *ACS Appl. Mater. Interfaces* **2014**, *6*, 5877−5883.
(37) Wei, N.; Peng, X.; Xu, Z. Breakdown of fast water transport in graphene oxides. *Phys. Rev. E* **2014**, *89*, 012113.
(38) Nair, R. R.; Wu, H. A.; Jayaram, P. N.; Grigorieva, I. V.; Geim, A. K. Unimpeded permeation of water through helium-leak-tight graphene-based membranes. *Science* **2012**, *335*, 442−444.
(39) Wei, N.; Lv, C.; Xu, Z. Wetting of graphene oxide: A molecular dynamics study. *Langmuir* **2014**, *30*, 3572−3578.
(40) Talyzin, A. V.; Hausmaninger, T.; You, S.; Szabó, T. The structure of graphene oxide membranes in liquid water, ethanol and water−ethanol mixtures. *Nanoscale* **2014**, *6*, 272−281.
(41) Joshi, R. K.; Carbone, P.; Wang, F. C.; Kravets, V. G.; Su, Y.; Grigorieva, I. V.; Wu, H. A.; Geim, A. K.; Nair, R. R. Precise and ultrafast molecular sieving through graphene oxide membranes. *Science* **2014**, *343*, 752−754.
(42) Qiu, L.; Zhang, X.; Yang, W.; Wang, Y.; Simon, G. P.; Li, D. Controllable corrugation of chemically converted graphene sheets in water and potential application for nanofiltration. *Chem. Commun.* **2011**, *47*, 5810−5812.
(43) Hung, W. S.; An, Q. F.; De Guzman, M.; Lin, H. Y.; Huang, S. H.; Liu, W. R.; Hu, C. C.; Lee, K. R.; Lai, J. Y. Pressure-assisted self-assembly technique for fabricating composite membranes consisting of highly ordered selective laminate layers of amphiphilic graphene oxide. *Carbon* **2014**, *68*, 670−677.
(44) Sun, P. Z.; Zhu, M.; Wang, K. L.; Zhong, M. L.; Wei, J. Q.; Wu, D. H.; Xu, Z. P.; Zhu, H. W. Selective ion penetration of graphene oxide membranes. *ACS Nano* **2013**, *7*, 428−437.
(45) Sun, P. Z.; Zheng, F.; Zhu, M.; Song, Z. G.; Wang, K. L.; Zhong, M. L.; Wu, D. H.; Little, R. B.; Xu, Z. P.; Zhu, H. W. Selective trans-membrane transport of alkali and alkaline earth cations through graphene oxide membranes based on cation-pi interactions. *ACS Nano* **2014**, *8*, 850−859.
(46) Rulíšek, L.; Havlas, Z. Theoretical studies of metal ion selectivity. 2. DFT calculations of complexation energies of selected transition metal ions (Co^{2+}, Ni^{2+}, Cu^{2+}, Zn^{2+}, Cd^{2+}, and Hg^{2+}) in metal-binding sites of metalloproteins. *J. Phys. Chem. A* **2002**, *106*, 3855−3866.
(47) Park, S.; Lee, K. S.; Bozoklu, G.; Cai, W.; Nguyen, S. T.; Ruoff, R. S. Graphene oxide papers modified by divalent ions-enhancing mechanical properties via chemical cross-linking. *ACS Nano* **2008**, *2*, 572−578.
(48) Sun, P.; Wang, K.; Wei, J.; Zhong, M.; Wu, D.; Zhu, H. Effective recovery of acids from iron-based electrolytes using graphene oxide membrane filters. *J. Mater. Chem. A* **2014**, *2*, 7734−7737.
(49) Coleman, M.; Tang, X. S. Diffusive transport of two charge equivalent and structurally similar ruthenium complex ions through graphene oxide membranes. *Nano Res.* **2015**, *8*, 1128−1138.
(50) Huang, H.; Mao, Y.; Ying, Y.; Liu, Y.; Sun, L.; Peng, X. Salt concentration, pH and pressure controlled separation of small molecules through lamellar graphene oxide membranes. *Chem. Commun.* **2013**, *49*, 5963−5965.
(51) Huang, H. B.; Song, Z. G.; Wei, N.; Shi, L.; Mao, Y. Y.; Ying, Y. L.; Sun, L. W.; Xu, Z. P.; Peng, X. S. Ultrafast viscous water flow through nanostrand-channelled graphene oxide membranes. *Nat. Commun.* **2013**, *4*, 2979.
(52) Wang, W.; Eftekhari, E.; Zhu, G.; Zhang, X.; Yan, Z.; Li, Q. Graphene oxide membranes with tunable permeability due to embedded carbon dots. *Chem. Commun.* **2014**, *50*, 13089−13092.

DOI: 10.1021/acs.iecr.6b00620
Ind. Eng. Chem. Res. 2016, 55, 4803−4810

(53) Li, W.; Zhang, Y.; Xu, Z.; Yang, A.; Meng, Q.; Zhang, G. Self-assembled graphene oxide microcapsules with adjustable permeability and yolk−shell superstructures derived from atomized droplets. *Chem. Commun.* **2014**, *50*, 15867−15869.
(54) Jia, Z.; Wang, Y. Covalently crosslinked graphene oxide membranes by esterification reactions for ions separation. *J. Mater. Chem. A* **2015**, *3*, 4405−4412.
(55) Stankovich, S.; Dikin, D. A.; Piner, R. D.; Kohlhaas, K. A.; Kleinhammes, A.; Jia, Y.; Wu, Y.; Nguyen, S. T.; Ruoff, R. S. Synthesis of graphene-based nanosheets via chemical reduction of exfoliated graphite oxide. *Carbon* **2007**, *45*, 1558−1565.
(56) Li, D.; Mueller, M. B.; Gilje, S.; Kaner, R. B.; Wallace, G. G. Processable aqueous dispersions of graphene nanosheets. *Nat. Nanotechnol.* **2008**, *3*, 101−105.
(57) Zhang, J.; Yang, H.; Shen, G.; Cheng, P.; Zhang, J.; Guo, S. Reduction of graphene oxide via L-ascorbic acid. *Chem. Commun.* **2010**, *46*, 1112−1114.
(58) Fernandez-Merino, M. J.; Guardia, L.; Paredes, J. I.; Villar-Rodil, S.; Solis-Fernandez, P.; Martinez-Alonso, A.; Tascon, J. M. D. Vitamin C is an ideal substitute for hydrazine in the reduction of graphene oxide suspensions. *J. Phys. Chem. C* **2010**, *114*, 6426−6432.
(59) Zhou, X.; Zhang, J.; Wu, H.; Yang, H.; Zhang, J.; Guo, S. Reducing graphene oxide via hydroxylamine: A simple and efficient route to graphene. *J. Phys. Chem. C* **2011**, *115*, 11957−11961.
(60) Pei, S.; Zhao, J.; Du, J.; Ren, W.; Cheng, H. M. Direct reduction of graphene oxide films into highly conductive and flexible graphene films by hydrohalic acids. *Carbon* **2010**, *48*, 4466−4474.
(61) Mei, X.; Meng, X.; Wu, F. Hydrothermal method for the production of reduced graphene oxide. *Phys. E* **2015**, *68*, 81−86.
(62) Chua, C. K.; Pumera, M. Chemical reduction of graphene oxide: A synthetic chemistry viewpoint. *Chem. Soc. Rev.* **2014**, *43*, 291−312.
(63) Pei, S.; Cheng, H. M. The reduction of graphene oxide. *Carbon* **2012**, *50*, 3210−3228.
(64) Gao, J.; Liu, F.; Liu, Y.; Ma, N.; Wang, Z.; Zhang, X. Environment-friendly method to produce graphene that employs vitamin C and amino acid. *Chem. Mater.* **2010**, *22*, 2213−2218.
(65) Thakur, S.; Karak, N. Alternative methods and nature-based reagents for the reduction of graphene oxide: A review. *Carbon* **2015**, *94*, 224−242.
(66) Su, Y.; Kravets, V. G.; Wong, S. L.; Waters, J.; Geim, A. K.; Nair, R. R. Impermeable barrier films and protective coatings based on reduced graphene oxide. *Nat. Commun.* **2014**, *5*, 4843.
(67) Liu, H.; Wang, H.; Zhang, X. Facile fabrication of freestanding ultrathin reduced graphene oxide membranes for water purification. *Adv. Mater.* **2015**, *27*, 249−254.
(68) Sun, P. Z.; Chen, Q.; Li, X. D.; Liu, H.; Wang, K. L.; Zhong, M. L.; Wei, J. Q.; Wu, D. H.; Ma, R. Z.; Sasaki, T.; Zhu, H. Highly efficient quasi-static water desalination using monolayer graphene oxide/titania hybrid laminates. *NPG Asia Mater.* **2015**, *7*, e162.
(69) Sasaki, T.; Watanabe, M.; Hashizume, H.; Yamada, H.; Nakazawa, H. Macromolecule-like aspects for a colloidal suspension of an exfoliated titanate. Pairwise association of nanosheets and dynamic reassembling process initiated from it. *J. Am. Chem. Soc.* **1996**, *118*, 8329−8335.
(70) Wang, L.; Sasaki, T. Titanium oxide nanosheets: graphene analogues with versatile functionalities. *Chem. Rev.* **2014**, *114*, 9455−9486.
(71) Zhang, M.; Gao, B.; Chen, J.; Li, Y.; Creamer, A. E.; Chen, H. Slow-release fertilizer encapsulated by graphene oxide films. *Chem. Eng. J.* **2014**, *255*, 107−113.
(72) Zhao, J.; Wang, Z.; White, J. C.; Xing, B. Graphene in the aquatic environment: adsorption, dispersion, toxicity and transformation. *Environ. Sci. Technol.* **2014**, *48*, 9995−10009.
(73) Sanchez, V. C.; Jachak, A.; Hurt, R. H.; Kane, A. B. Biological interactions of graphene-family nanomaterials: An interdisciplinary review. *Chem. Res. Toxicol.* **2012**, *25*, 15−34.
(74) Zhang, H.; Peng, C.; Yang, J.; Lv, M.; Liu, R.; He, D.; Fan, C.; Huang, Q. Uniform ultrasmall graphene oxide nanosheets with low cytotoxicity and high cellular uptake. *ACS Appl. Mater. Interfaces* **2013**, *5*, 1761−1767.
(75) Hu, W.; Peng, C.; Luo, W.; Lv, M.; Li, X.; Li, D.; Huang, Q.; Fan, C. Graphene-based antibacterial paper. *ACS Nano* **2010**, *4*, 4317−4323.
(76) Lv, M.; Zhang, Y.; Liang, L.; Wei, M.; Hu, W.; Li, X.; Huang, Q. Effect of graphene oxide on undifferentiated and retinoic acid-differentiated SH-SY5Y cells line. *Nanoscale* **2012**, *4*, 3861−3866.
(77) Stankovich, S.; Dikin, D. A.; Compton, O. C.; Dommett, G. H.; Ruoff, R. S.; Nguyen, S. T. Systematic post-assembly modification of graphene oxide paper with primary alkylamines. *Chem. Mater.* **2010**, *22*, 4153−4157.
(78) Yeh, C. N.; Raidongia, K.; Shao, J.; Yang, Q. H.; Huang, J. On the origin of the stability of graphene oxide membranes in water. *Nat. Chem.* **2015**, *7*, 166−170.
(79) Sun, S.; Wang, C.; Chen, M.; Li, M. The mechanism for the stability of graphene oxide membranes in a sodium sulfate solution. *Chem. Phys. Lett.* **2013**, *561-562*, 166−169.
(80) Hung, W. S.; Tsou, C. H.; De Guzman, M.; An, Q. F.; Liu, Y. L.; Zhang, Y. M.; Hu, C. C.; Lee, K. R.; Lai, J. Y. Cross-linking with diamine monomers to prepare composite graphene oxide-framework membranes with varying *d*-spacing. *Chem. Mater.* **2014**, *26*, 2983−2990.
(81) Xu, K.; Feng, B.; Zhou, C.; Huang, A. Synthesis of highly stable graphene oxide membranes on polydopamine functionalized supports for seawater desalination. *Chem. Eng. Sci.* **2016**, *146*, 159−165.
(82) Han, Y.; Xu, Z.; Gao, C. Ultrathin graphene nanofiltration membrane for water purification. *Adv. Funct. Mater.* **2013**, *23*, 3693−3700.

DOI: 10.1021/acs.iecr.6b00620
Ind. Eng. Chem. Res. 2016, 55, 4803−4810